

# Numerical Investigation of a Marine Two-Stroke Diesel Engine Using the Eddy Dissipation Concept with NO- and Auto-Ignition Model

N.I.Lilleheie and E.Pedersen\*

*SINTEF Applied Thermodynamics  
Kolbj. Hejes v. 1 B, N-7031 Trondheim  
Norway*

\* *MARINTEK Machinery*

## Abstract

The optimization of marine diesel engines is necessary in order to increase the thermal efficiency (reduction of the CO<sub>2</sub> emission) and reduction of soot and NO<sub>x</sub> emissions. This optimization may be economized by using numerical field simulations to get a good first estimate of the geometrical and operational design that should be used. Such simulations provide detailed information about the combustion process where the major limitations are the accuracy of the mathematical models and the numerical scheme.

The KIVA-II code has been used to simulate a medium speed two stroke marine diesel engine. The code is specially designed to follow the piston movement of an engine (the ALE - method) and a Lagrangian spray model where breakup, coalescence and evaporation are included.

The code has been extended with the Eddy Dissipation Concept of Magnussen to handle turbulent combustion. In addition the Zeldovich mechanism for NO<sub>x</sub> formation, the soot model according to Magnussen and an auto-ignition model according to Theobald has been implemented in the code.

Simulated fields of temperature, CO, CO<sub>2</sub> and NO are presented. In addition computational results are shown for rate of heat release, pressure, temperature, CO, NO and soot concentration as a function of crank angle. The results for pressure and heat release are compared with experimental result. Also exhaust NO, CO and CO<sub>2</sub> levels are compared with experiments.

## Introduction

Detailed knowledge about the different processes in a diesel engine is crucial in order to make improvement of the overall process. This knowledge is obtainable by solving the governing equations for conservation of mass, momentum and energy. This is however a huge task due to the turbulent flow pattern in an engine, and modeling concepts must be applied in order to close the set of averaged governing equations.

The models as such resides on certain assumptions about the physical processes, and the results from the computations where these models are used, must be evaluated with the limitations embodied in the assumptions as restrictions on the validity of the results.

With these restriction laid on our computational efforts, useful information may be extracted from the nu-

merical results, and the influence of initial conditions and geometrical constraints on the different process parameters can be obtained. Restricted by the same modeling limitations, detailed information about the origin of the change in process parameters can be identified, and a guidance to experimental verification of the observed phenomena is obtained.

## The numerical code

The numerical code applied is the KIVA-II code of the Los Alamos Laboratories [1]. This code consist of a Lagrangian spray model and an arbitrary Lagrangian-Eulerian control volume model for the gas phase.

The spray model used is the conventional KIVA-II model where the breakup, collision and random influence of turbulence on the droplets are neglected. The droplets are injected with a given initial radial  $\xi$ -squared distribution. The Sauter Mean Radius (SMR) of the injected particles was set to 24  $\mu$ .

The gas phase model of KIVA-II code contains models for mass, average momentum, turbulence momentum (the  $k - \epsilon$  model), internal energy and specific densities for the species. The code is also provided with routines for chemical conversion, but these are based on average quantities for temperature and species mole fractions. This is not a physical correct picture of chemical conversion in turbulent reacting flow. Based on this the KIVA-II code has been extended with a turbulent combustion model, the "Eddy Dissipation Concept" (EDC) of Magnussen [2]. In addition the soot model of Magnussen [3], NO formation analog to the EDC using the Zeldovich mechanism [4] and an auto-ignition model according to the Theobald extension of the Shell knock model [5] are implemented into the code.

## Combustion and soot modeling

The combustion model used is the "Eddy Dissipation Concept" (EDC) of Magnussen [2]. This model is based on that the heat releasing chemical reactions take place in the intermittently distributed dissipating fine structures of turbulence. The mixing in the dissipative structures are assumed to be fast, and as a consequence, the combustion in the burning fine structures is modeled as perfectly stirred reactors.

Taking into consideration that only a fraction,  $\chi$ ,

of the fine structures are burning [2], we can relate the mean density to the fine structures and the surroundings as follows:

$$\frac{1}{\bar{\rho}} = \frac{\gamma^* \chi}{\rho^*} + \frac{1 - \gamma^* \chi}{\rho^0} \quad (1)$$

where \* represent the burning fine structures and <sup>0</sup> represents the fine structure surroundings.  $\gamma^*$  is the intermittency factor for the burning fine structures [2]. Density weighted mass fractions will then be given as

$$\tilde{Y}_i = \gamma^* \chi Y_i^* + (1 - \gamma^* \chi) Y_i^0 \quad (2)$$

The governing equation for the reacting fine structures, modeled as perfectly stirred reactors are given as:

$$\frac{dY_i^*}{dt} + \frac{\dot{m}^*}{1 - \chi \gamma^*} (Y_i^* - \tilde{Y}_i) = \dot{R}_i^* \quad (3)$$

$$\frac{dh^*}{dt} + \frac{\dot{m}^*}{1 - \chi \gamma^*} (h^* - \tilde{h}) = \frac{1}{\rho^*} \frac{dP}{dt} \quad (4)$$

where  $\dot{R}_i^*$  is the reaction rate of species  $i$ ,  $P$  is the pressure and  $\dot{m}^*$  is the mass exchange rate between the burning fine structures and its surroundings [2]. The pressure term is neglected in this work. The mean reaction rate is given by:

$$\bar{R}_i = \gamma^* \chi \dot{R}_i^* \quad (5)$$

The currently implemented EDC operates on conversion of fuel and  $O_2$  to CO and  $H_2$  which equilibrates with  $CO_2$ ,  $H_2$  and  $O_2$ .

The soot model is also according to Magnussen and is based on the soot formation model of Tesner [6] applied in turbulent combustion according to the EDC [3].

The soot model is a two variable model; nucleus for soot growth,  $Y_n$ , and soot,  $Y_{soot}$ . The balance equation for soot and nucleus in the fine structures are given by:

$$\frac{dY_n^*}{dt} + \frac{\dot{m}^*}{1 - \chi \gamma^*} (Y_n^* - \tilde{Y}_n) = \dot{R}_{f,n}^* + \dot{R}_{c,n}^* \quad (6)$$

$$\frac{dY_s^*}{dt} + \frac{\dot{m}^*}{1 - \chi \gamma^*} (Y_s^* - \tilde{Y}_s) = \dot{R}_{f,s}^* + \dot{R}_{c,s}^* \quad (7)$$

where  $\dot{R}_f^*$  and  $\dot{R}_c^*$  are formation and combustion rates. The transient terms are omitted in this work.

The formation and destruction terms are described by Magnussen [3].

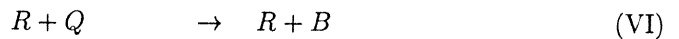
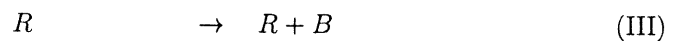
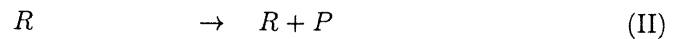
## The auto-ignition model

The ignition delay is modeled by using the extension of the Shell knocking model as reported by Theobald [5].

The Shell knocking model identifies three types of species which is important for onset of auto-ignition in hydrocarbons:

- $R$  - Reactive radicals
- $B$  - Branching species which splits into two radicals.
- $Q$  - Intermediate species which are formed from the radicals and generates branching species

The following types of reactions are identified:



where  $P$  is combustion product.

The implementation of this model is mainly according to Theobald, but a few changes have been made. The termination reactions are not assumed to produce  $N_2$  but  $CO_2$  and  $H_2O$ , and in addition we have used a slightly different integration method for the chemical source terms. In the original KIVA-II code, the chemical reactions are solved in order to obtain detailed mass balance for each reaction and in addition prevent species from being driven negative. The way this is handled in KIVA on a quasi implicit basis, results in different degree of implicitness for the different reactions. This is not to be recommended, so an alternative method where the same degree of implicitness is applied to all reactions is used, but still demanding mass balance to be fulfilled. To prevent the overall time step to become intractable small, sub-cycling on the integration of the chemical reactions is applied.

The Shell knocking model is able to predict two stage ignition. For onset of auto-ignition under diesel engine like condition, the two stage ignition is not dominant. The onset of one stage ignition is governed by the conversion of intermediate species,  $Q$ , to the branching species,  $B$  [5]. The conversion of  $Q$  to  $B$  is governed by reaction (VI). In addition, the onset of one-stage ignition is dependent on the initiation reaction (I).

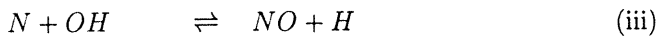
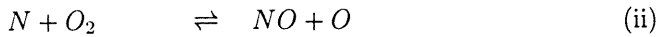
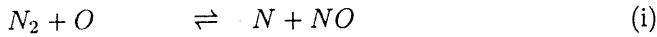
The implementation is tested versus the computational results of Theobald for auto-ignition of 90 RON fuel. Our result were in agreement with the results of Theobald.

The fuel used in the experiment was a typical gas-diesel fuel with a C/H ratio of 1.85. The physical properties of the fuel was put equal to dodecan, and the parameters of the Shell model which Theobald used, were found to be applicable for this case to.

## The NO<sub>x</sub> model

The high process temperature in the diesel engine indicates that the Zeldovich mechanism [4] is a sufficient chemical kinetic mechanism to describe the NO formation in the diesel engine process.

The extended Zeldovich mechanism is given by:



By assuming steady state condition for the  $N$  atoms the following expression for the NO reaction rate is found.

$$\frac{d[NO]}{dt} = 2k_{if}[O][N_2] \cdot \frac{\left\{ 1 - \frac{1}{K_{Ci} \cdot K_{Cii}} \frac{[NO]^2}{[O_2][N_2]} \cdot \frac{\left(1 + \frac{k_{iib}}{k_{iif}} \cdot \frac{[H]}{[O]}\right)}{\left(1 + \frac{k_{iif}}{k_{iif}} \cdot \frac{[OH]}{[O_2]}\right)} \right\}}{\left\{ 1 + \frac{k_{iib}[NO]}{(k_{iif}[O_2] + k_{iif}[OH])} \right\}} \quad (8)$$

where  $K_{Ci}$  and  $K_{Cii}$  is the equilibrium constants for reaction (i) and (ii)

In order to make the model work without knowledge about OH, O and H levels, the following assumptions are made:

- I The O atoms are in equilibrium with O<sub>2</sub>.
- II The denominator of eq. (8) equals one.
- III The last fraction of the second term of the nominator in eq. (8) equals 1.

This gives the following reaction rate:

$$\frac{d[NO]}{dt} = 2k_{if}[O][N_2] \cdot \left\{ 1 - \frac{1}{K_{Ci} \cdot K_{Cii}} \frac{[NO]^2}{[O_2][N_2]} \right\} \quad (9)$$

The assumptions II and III are made in order to improve the simplest expression for the NO reaction rate based on the Zeldovich mechanism. This reaction rate involves only the first term of eq. (8) and hence neglects any dissociation of NO into N<sub>2</sub> and O<sub>2</sub>.

The validity of the assumptions II and III are tested for perfectly stirred reactor calculations using detailed chemistry under engine-like conditions. These tests show that the assumptions are sufficient correct for lean and stoichiometric conditions, and always better than the simplest version of the NO reaction rate.

## Computational results

The computational results are from simulations of a two-stroke medium range marine diesel engine from Wärtsilä Wichmann, Norway, which are experimentally investigated at MARINTEK Machinery [7]. The engine stroke is 360mm, the cylinder diameter is 280mm and the injector is located in center of the head with ten 0.15mm diameter

nozzles. The injection angle was 67.5° from the center of the cylinder.

In the simulations the cylinder was represented by a 36° sector which is the smallest sector with geometrical symmetry. This sector was resolved in 7 computational sectors divided into 42 annuli along the diameter of the cylinder. At TDC the distance between piston top and the engine head was divided into 12 levels.

Four different cases was simulated: 1) 25 % load with 380 rpm, 2) 50 % load with 475 rpm, 3) 100 % load with 600 rpm and 4) 100 %load with 720 rpm.

The detailed information of field simulations are instructive in order to see if assumed connection between different variables exists. Planes through the computational field are shown in fig. (1) for temperature and velocity, CO, CO<sub>2</sub> and NO 9° ATDC. The shape of the flame are clearly illustrated by the velocity field onset by the momentum from the diesel spray. The flow field shows a recirculation zone in the middle of the flame which also is a high temperature region. This indicates that the flow transports hot products into the recirculation zone. This is confirmed by the CO<sub>2</sub> field.

The CO field shows highest concentrations in the front of the jet generated by the spray. The high CO level may be a result of poor mixing and hence, only small amounts of O<sub>2</sub> are mixed with the fuel. The maximum CO level coincide with low CO<sub>2</sub> levels. This coincident is equivalent to rich conditions where not enough O<sub>2</sub> are present to convert fuel to CO<sub>2</sub>.

The NO field shows maximum values in the region of high temperature which is correct according to the thermal NO model used.

The rate of heat release of case 1) - 3) is shown in fig. (2). The irregularity of the computed results are due to the non-uniform distribution of the droplets in the computations, and hence the evaporation will not occur smooth. The computational results reflects the shifting of the heat release with crank angle as shown by the experiment. The rate of heat release calculations from the field simulations gives satisfactory onset of ignition.

The process pressure of case 1) - 3) is shown in fig. (3). The computed results are in very good agreement with the experiments, and indicates a satisfactory description of the heat releasing process in the computations.

The process temp of case 1) - 3) is shown in fig. (4). The temperature is found to be higher for the 50 % load than for the 25 % load and the 100 % load. An explanation might be that for the 25 % load, the excess air will lower the temperature considerably while for the 100 % load the combustion process are not completed before the expansion stroke has started to affect the temperature. This is due to the longer injection period for case 3).

The CO mass fraction of case 1) - 3) is shown in fig. (5). The variation reflects to some extent the variation in temperature. The major effect on the CO level is the dissociation at high temperatures, which also explain the difference between case 1) and 2). For case 3), the maximum level is almost as high as for case 2). This may

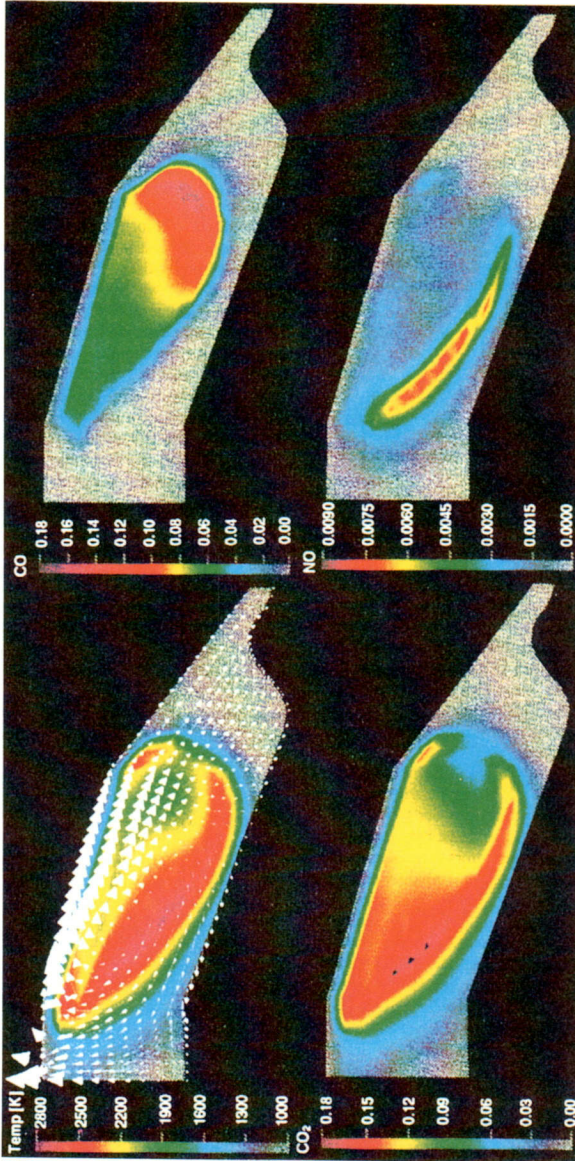


Figure 1: Temperature, velocity, CO mass fraction and CO<sub>2</sub> mass fraction fields on a plane through the middle of a 36° sector of the cylinder - Crank angle = 9° ATDC

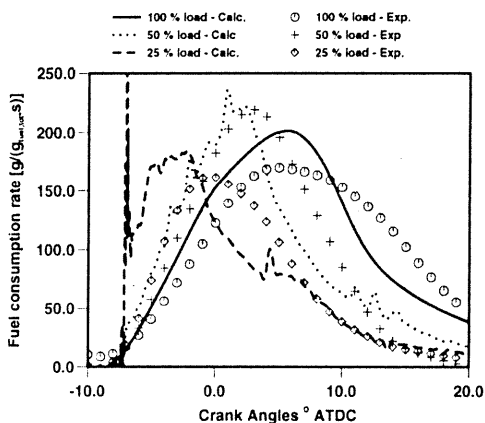


Figure 2: The rate of heat release for 25 %, 50 % and 100 % load compared with experiments

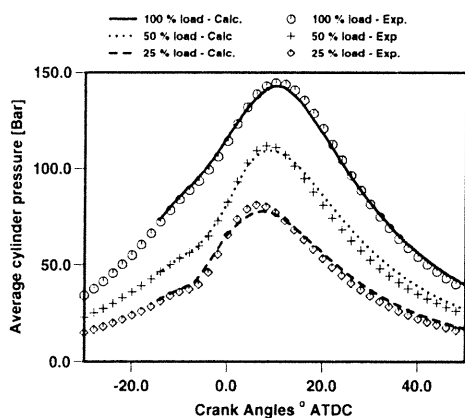


Figure 3: The process pressure for 25 %, 50 % and 100 % load compared with experiments

be explained with the lower air/fuel ratio for case 3) which prevent CO oxidation.

The soot mass fraction of case 1) - 3) is shown in fig. (6). The development of the soot mass fraction is clearly seen to follow the behavior of the temperature. The process curve of soot are more peaked than the temperature curve. The spontaneous formation of soot nucleus is modeled as an Arrhenius expression according to Tesner [6] which explain the consistency with the temperature variation. The soot reduction shown is due to soot combustion.

The NO mass fraction of case 1) - 3) is shown in fig. (7). The consistency with the temperature variation is again pronounced. The difference between case 1) and 3) is larger than for the temperature. This may be explained by the NO formation dependency on O<sub>2</sub>. For case 1) the air/fuel ratio is larger than for case 3) and will therefore promote the NO formation. The stable level of the NO mass fraction results from the strongly temperature dependent dissociation process of NO to O<sub>2</sub> and N<sub>2</sub>.

Calculated outlet values of different species for case 1) - 4) are compared with experimental findings and given

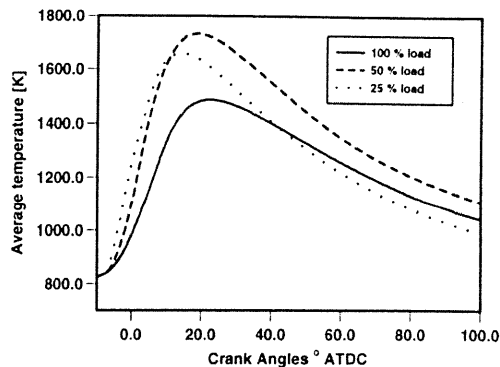


Figure 4: The process temperature for 25 %, 50 % and 100 % load

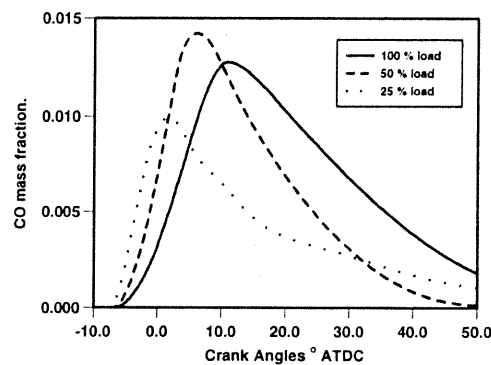


Figure 5: The CO mass fraction for 25 %, 50 % and 100 % load

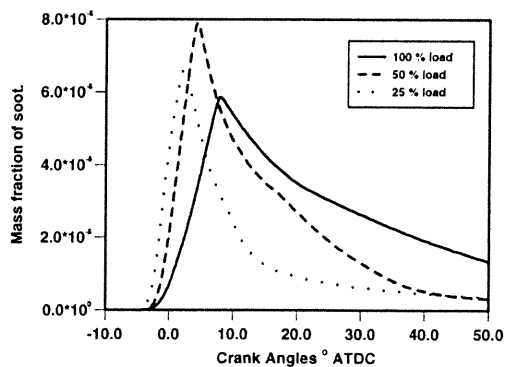


Figure 6: The soot mass fraction for 25 %, 50 % and 100 % load.

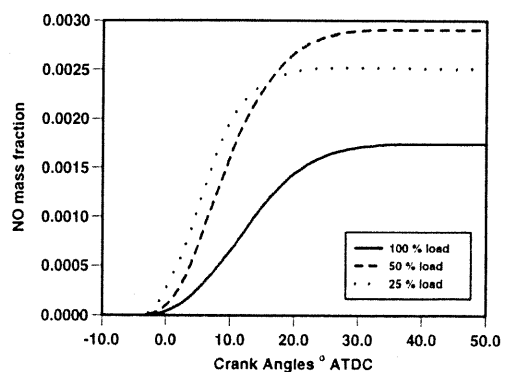


Figure 7: The NO mass fraction for 25 %, 50 % and 100 % load

Table 1: Outlet levels of different species for 1) 25 % load, 2) 50 % load, 3) 100 % load and 4) 100 % load with 20 % increase in engine speed

	CO <sub>2</sub> [kg/kg <sub>fuel</sub> ]		CO [g/kg <sub>fuel</sub> ]		NO [g/kg <sub>fuel</sub> ]	
	Exp.	Calc.	Exp.	Calc.	Exp.	Calc.
1	3.5	3.2	2.8	6.7	92.0	100.0
2	3.3	3.2	31.5	2.0	77.0	99.0
3	3.4	3.2	7.5	1.8	59.8	68.2
4	3.3	3.2	8.8	1.9	44.4	48.0

in table (1). The CO<sub>2</sub> level is correctly reproduced within 10 % of the experimental results which again shows that the overall heat release is correctly modeled. The CO level is not well simulated compared with the experimental findings. This may be explained with the fact that equilibrium was assumed in the reaction zones and therefore kinetic effects which may affect the CO level are neglected. The NO level is somewhat over-predicted but within 30 % of the experimental findings. What is more important is the qualitatively behavior of the simulations which shows the same trend as the experiments when changing the load and the engine speed.

## Conclusions

The KIVA-II code has been provided with models for auto-ignition, turbulent combustion, soot- and NO formation. The computational results show good agreement with experiments on a medium range two-stroke marine diesel engine for the onset of ignition, heat release and NO formation. The CO level is not well predicted using equilibrium assumption in the reaction zones and chemical kinetic effects on CO formation should be incorporated in the CO model.

The simulations show expected coincidence between the different variables and the code seems to be a good tool for testing the effect of different load and engine speed on the NO emission.

## Acknowledgements

This work is carried out at MARINTEK A/S, the Norwegian Marine Technology Research Institute A/S, within the research project "Environmental Friendly Diesel Engines - Development of Basic Knowledge". The authors thanks ESSO Norge A/S, MARINTEK A/S and the Research Council of Norway for supporting this work.

## References

- [1] Amsden, A.A., O'Rourke, P.J. and Butler, T.D., "KIVA-II: A Computer Program for Chemically Reactive Flows with Spray," LA-11560-MS, Los Alamos National Laboratory, New Mexico, 1989
- [2] Magnussen, B.F., "The Eddy Dissipation Concept," XI Task Leaders Meeting - Energy Conservation in Combustion, IEA, pp 248-268, 1989.
- [3] Magnussen, B.F., "Modeling of Reaction Processes in Turbulent Flames with Special Emphasis on Soot Formation and Combustion," Particulate Carbon Formation During Combustion (Siegla and Smith ed.) Plenum Publishing Corporation, pp 321-341, 1981.
- [4] Miller, J.A. and Bowman, C.T., "Mechanism and Modeling of Nitrogen Chemistry in Combustion," Prog. Energy and Combust. Sci., vol. 15, pp 287-338, 1989.
- [5] Theobald, M.A., "A Numerical Simulation of Diesel Autoignition", Ph.D. Thesis, Dep. of Mech. Eng., Massachusetts Institute of Technology, 1986.
- [6] Tesner, P.A., Snegiriova, T.D. and Knorre, V. G., Combustion and Flame, 17,2, pp 253-260, 1971.
- [7] Småvik, M.B., MARINTEK report, MARINTEK Norway, MT22-F94-0022, (in norwegian), 1994